Plasma fibronectin deficiency impedes atherosclerosis progression and fibrous cap formation

Ina Rohwedder[1†], Eloi Montanez[1,2†], Karsten Beckmann[1,‡], Eva Bengtsson[3], Pontus Dunér[3], Jan Nilsson[3], Oliver Soehnlein[4], Reinhard Fässler[1]*

Keywords: atherosclerosis; fibronectin; fibrous cap; inflammation; migration

DOI 10.1002/emmm.201200237

Received September 23, 2011
Revised February 29, 2012
Accepted March 01, 2012

→See accompanying article
http://dx.doi.org/10.1002/emmm.201200238

Atherosclerotic lesions are asymmetric focal thickenings of the intima of arteries that consist of lipids, various cell types and extracellular matrix (ECM). These lesions lead to vascular occlusion representing the most common cause of death in the Western world. The main cause of vascular occlusion is rupture of atheromatous lesions followed by thrombus formation. Fibronectin (FN) is one of the earliest ECM proteins deposited at atherosclerosis-prone sites and was suggested to promote atherosclerotic lesion formation. Here, we report that atherosclerosis-prone apolipoprotein E-null mice lacking hepatocyte-derived plasma FN (pFN) fed with a pro-atherogenic diet display dramatically reduced FN depositions at atherosclerosis-prone areas, which results in significantly smaller and fewer atherosclerotic plaques. However, the atherosclerotic lesions from pFN-deficient mice lacked vascular smooth muscle cells and failed to develop a fibrous cap. Thus, our results demonstrate that while FN worsens the course of atherosclerosis by increasing the atherogenic plaque area, it promotes the formation of the protective fibrous cap, which in humans prevents plaques rupture and vascular occlusion.

INTRODUCTION

Atherosclerosis is a progressive inflammatory disease of large arteries characterized by an accumulation of lipids and extracellular matrix (ECM) proteins in the affected vessel wall (Lusis, 2000). Atherosclerosis commences with the deposition of lipoprotein particles into the subendothelial matrix and the recruitment of monocytes to the luminal surface of the endothelium. Next, monocytes transmigrate across the endothelial monolayer into the intima, where they proliferate and differentiate into macrophages that take up the lipoprotein particles and form foam cells (Woollard & Geissmann, 2010). Finally, macrophage-derived chemoattractants induce the migration of vascular smooth muscle cells (vSMC) from the vessel wall into the lesion, where they secrete ECM proteins resulting in lesion growth and the formation of the 'fibrous cap' that encloses the lipid-rich core (Newby & Zaltsman, 1999). The rupture of fibrous caps represents an injured vessel surface and triggers adhesion and activation of platelets, which can culminate in thrombus formation and eventually myocardial infarction or stroke (Lusis, 2000). Therefore, the rupture of an atherosclerotic plaque always represents a life-threatening event. Plaque rupture depends on many factors including the composition and vulnerability of plaques (Lusis, 2000). Vulnerable plaques have thin fibrous caps and contain elevated numbers of inflammatory cells (Newby, 2007; Newby et al, 2009).

(1) Department for Molecular Medicine, Max Planck Institute of Biochemistry, Martinsried, Germany
(2) Walter-Brendel-Centre of Experimental Medicine, Ludwig-Maximilians University Munich, Munich, Germany
(3) Department of Clinical Sciences Malmö, Skåne University Hospital, Lund University, Malmö, Sweden
(4) Institute for Cardiovascular Prevention (IPEK), Ludwig-Maximilians University Munich, Munich, Germany
***Corresponding author:** Tel: +49 89 85782424; Fax: +49 89 85782422; E-mail: Faessler@biochem.mpg.de

†These authors contributed equally to this work.
‡Present address: U3 Pharma GmbH, Martinsried, Germany

Despite the systemic nature of atherosclerotic risk factors, which comprise hypercholesterolemia, hyperglycemia, obesity and smoking, atherosclerotic lesions develop preferentially at vessel curvatures, branching points and bifurcations, where the blood flow is highly turbulent (Hahn & Schwartz, 2009). *In vitro* studies suggested that the turbulent blood flow at these atherosclerotic-prone sites exerts mechanical forces on endothelial cells (EC) leading to the activation of EC integrins, the secretion and deposition of fibronectin (FN) (Feaver et al, 2010) and the activation of inflammatory mediators such as NF-κB, the c-Jun NH2-terminal kinases (JNKs) and p21-activated kinase (PAK) (Funk et al, 2010; Hahn & Schwartz, 2008; Hahn et al, 2009; Orr et al, 2005, 2007, 2008). These mediators induce endothelial permeability, sustain an inflammatory state and thereby enforce the consequences of the turbulent blood flow during atherogenesis (Hahn et al, 2009; Orr et al, 2005, 2007).

FNs are a family of large ECM proteins that are generated by alternative splicing from a single gene. FN is found in all vertebrates where it exists in two different forms; one form is cellular FN (cFN), which contains, depending on the tissue, variable proportions of the alternatively spliced exons coding for the extra domains A and B (EDA, EDB). cFN is synthesized and secreted by many cells and assembled into an insoluble fibrillar matrix. The other form is plasma FN (pFN), which lacks EDA and EDB. pFN is synthesized by hepatocytes and released into the circulation where it remains soluble (Leiss et al, 2008; White et al, 2009). Assembly of FN into insoluble and biologically active fibrils critically depends on the interaction with integrins resulting in the unmasking of cryptic FN binding sites, association with other FN proteins and finally crosslinking by tissue transglutaminases into a fibrillar matrix (Hynes, 2002; Leiss et al, 2008). Soluble pFN can also be assembled into fibrils, however, only after it is bound by integrins, *e.g.* on platelets or after transfer into tissues (Moretti et al, 2007; Oh et al, 1981). Studies published more than 20 years ago showed that the expression of FN is elevated in vessel walls of atherosclerotic regions and, therefore, suggested a role for FN during the course of atherosclerosis (Glukhova et al, 1989). Deletion of the *FN* gene in mice leads to early embryonic lethality (George et al, 1993), which precludes the analysis of atherosclerosis. However, a specific ablation of the exon encoding the alternatively spliced EDA domain in atherosclerosis-prone mice was reported to reduce the number and size of atherosclerotic lesions, suggesting that the EDA domain in cFN supports atherogenesis (Babaev et al, 2008; Tan et al, 2004). In line with this observation, the expression of FN-EDA is high during atherosclerosis (Astrof & Hynes, 2009). A correlation between elevated pFN levels and increased incidence for atherosclerosis in human patients has been shown in some studies but also refuted in others (Orem et al, 2003; Ozcelik et al, 2009; Tzanatos et al, 2009; Vavalle et al, 2007; Zhang et al, 2006).

To elucidate the functions of pFN and monocyte/macrophage-derived FN in atherosclerosis, we used the Cre recombinase-loxP sites (*Cre-loxP*) system to delete the *FN* gene in either hepatocytes and/or haematopoietic cells of atherosclerosis-prone (ApoE)-null mice. While deleting *FN* in haematopoietic cells did not affect plaque formation, loss of pFN reduced FN deposits in the subendothelial space of atherosclerosis-prone regions and diminished the number and size of atherosclerotic lesions. Importantly, it also blocked the invasion of vSMCs and the formation of fibrous caps. Thus, pFN plays a dichotomous role in atherosclerosis: it promotes disease by supporting initiation and progression of atherosclerotic lesions but may prevent potential thrombotic events by promoting fibrous cap formation.

RESULTS

FN is deposited at atherosclerosis-prone sites

There are conflicting observations on a correlation of elevated pFN levels with an increased incidence for atherosclerosis in human patients (Orem et al, 2003; Ozcelik et al, 2009; Tzanatos et al, 2009; Vavalle et al, 2007; Zhang et al, 2006). To determine whether pFN plays a role during the course of the disease, we manipulated pFN expression in atherosclerosis-prone $ApoE^{-/-}$ mice using the *Cre-loxP* system. $ApoE^{-/-}$ mice subjected to a high-fat diet develop atherosclerotic lesions over the course of their lifespan (Nakashima et al, 1994). To first test whether FN accumulates at sites of disturbed flow in our model system, we induced atherosclerosis in 3-week-old $ApoE^{-/-}$ mice by feeding them for 12 weeks with a high-fat diet. Oil Red O staining of aortas and the vessels branching from the aortic arch (the innominate, the left common carotid and the left subclavian arteries) confirmed the formation of large, lipid-rich plaques at areas of disturbed blood flow in the innominate and subclavian arteries, and the lesser curvature of the aortic arch (Fig 1A). The Oil Red O-positive plaques were absent before subjecting $ApoE^{-/-}$ mice to the high-fat diet (Fig 1A). Furthermore, cross-sections revealed FN depositions in atherosclerosis-prone regions of aortic arches and innominate arteries, while cross-sections of regions of the aorta and the carotids protected from atherosclerosis did not show FN accumulations (Fig 1B).

Mx-Cre-mediated *FN* gene deletion reduced atherosclerotic plaque formation *in vivo*

Since FN depositions are particularly prominent in the subendothelial space and at the luminal surface of atherosclerosis-prone regions (Fig 1B), we hypothesized that soluble pFN is deposited at these sites and thus might play an important role in atherosclerosis. To test this hypothesis, we intercrossed $ApoE^{-/-}$ mice carrying a *loxP*-flanked *FN* gene ($ApoE^{-/-}FN^{fl/fl}$) with mice expressing the *Cre* recombinase under the control of the interferon- and polyinosinic-polycytidylic acid (poly-IC)-inducible *Mx* promoter (*Mx-Cre*) to produce $ApoE^{-/-}FN^{MxCre}$ mice. Deletion of the *FN* gene was induced in 2-week-old $ApoE^{-/-}FN^{MxCre}$ mice by a single intraperitoneal injection of poly-IC. Western blot (WB) analysis confirmed loss of pFN 1 week after the poly-IC injection (Fig 2A). Elimination of pFN was stable for at least 6 months. WB analysis of cell lysates from $ApoE^{-/-}FN^{MxCre}$ mice showed loss of FN expression in haematopoietic cells but neither in ECs nor in vSMCs from the aorta (Fig 2A and Supporting Information Fig 1A). Together, these results show that *Mx-Cre*-mediated deletion of the *FN* gene

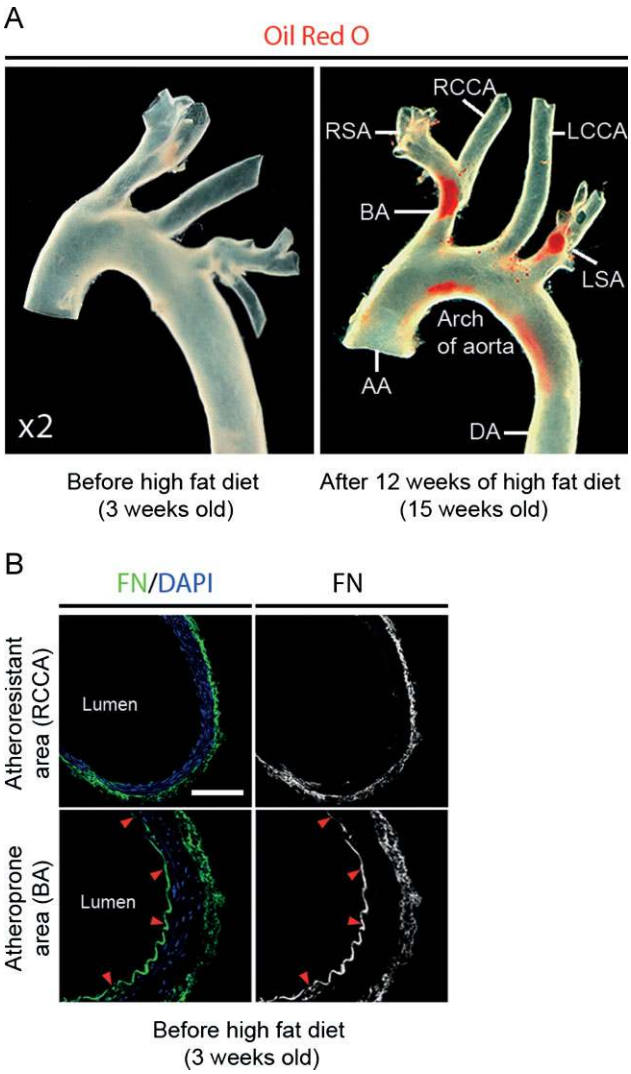

Figure 1. Fatty streaks and FN depositions at atherosclerosis-prone sites.

A. Whole-mount staining of Oil Red O of an aortic arch from ApoE$^{-/-}$ mice before and after feeding a high fat diet. AA, ascending aorta; BA, brachiocephalic artery; RSA, right subclavian artery; RCCA, right common carotid artery; LCCA, left common carotid artery; LSA, left subclavian artery; DA, descending aorta.

B. Immunostaining of FN of the aortic arch from ApoE$^{-/-}$ mice before the high fat diet. FN stains at the luminal side (arrow heads). Nuclei are visualized with DAPI. Scale bars represent 75 μm.

was efficient in hepatocytes and haematopoietic cells resulting in a complete and stable elimination of pFN in ApoE$^{-/-}$FN^{MxCre} mice.

To test whether loss of pFN affects development and/or progression of atherosclerosis, we subjected ApoE$^{-/-}$FN^{MxCre} and their control (ApoE$^{-/-}$FN$^{fl/fl}$) littermates to high-fat diet and performed whole-mount staining of longitudinally opened aortas with Oil Red O to visualize the lipid-rich atherosclerotic plaques. To avoid possible confounding effects of gender differences (Goldbourt & Neufeld, 1986), all experiments were performed with males. After 1 week of high-fat diet, none of the test groups displayed signs of atherosclerotic plaque formation. After 12 weeks of high fat diet, all mice developed atherosclerotic lesions with highest incidence at aortic arches and in the abdominal regions of the aorta (Fig 2B and Supporting Information Fig 1B). However, ApoE$^{-/-}$FN^{MxCre} mice showed significantly fewer atherosclerotic lesions when compared to ApoE$^{-/-}$FN$^{fl/fl}$ control littermates (Fig 2B–E). Quantitative analysis of Oil Red O-stained whole mount aortas revealed that ApoE$^{-/-}$FN^{MxCre} aortas displayed a 50% reduction of lesion areas (Fig 2C), which was due to significantly fewer (Fig 2D) as well as smaller lesions (Fig 2E). Altogether, these results indicate that *Mx-Cre*-mediated deletion of the *FN* gene protects against atherosclerosis.

Vav-Cre-mediated *FN* gene deletion in haematopoietic cells does not affect atherosclerosis

The *Mx-Cre* transgene is known to efficiently disrupt floxed genes in hepatocytes and haematopoietic cells. To determine whether ablation of the *FN* gene in haematopoietic cells including monocytes/macrophages affects the course of atherosclerosis, we intercrossed ApoE$^{-/-}$FN$^{fl/fl}$ mice with mice expressing the *Cre* recombinase under the control of the *Vav* promoter (*Vav-Cre*) to generate ApoE$^{-/-}$FN^{VavCre} mice. WB analysis of cell lysates from ApoE$^{-/-}$FN^{VavCre} mice showed loss of FN expression in haematopoietic cells but neither in hepatocytes nor in ECs and vSMCs from aorta (Fig 3A and unpublished observation). Consistent with normal *FN* gene activity in hepatocytes, ApoE$^{-/-}$FN^{VavCre} mice showed similar pFN levels as ApoE$^{-/-}$FN$^{fl/fl}$ control littermates (Fig 3A and Supporting Information Fig 1C).

Similar to ApoE$^{-/-}$FN$^{fl/fl}$ and ApoE$^{-/-}$FN^{MxCre} mice, ApoE$^{-/-}$FN^{VavCre} mice did not develop atherosclerotic lesions after 1 week of high-fat diet. However, after 12 weeks of a high-fat diet, ApoE$^{-/-}$FN^{VavCre} mice displayed atherosclerotic plaques at atherosclerosis-prone regions (Fig 3B). The overall areas covered with lesions as well as the atherosclerotic plaque sizes and numbers did not differ from those observed in ApoE$^{-/-}$FN$^{fl/fl}$ control littermates (Fig 3C–E). These findings indicate that FN derived from haematopoietic cells does not exert a major impact on the development of atherosclerosis.

Loss of pFN reduced FN deposition at atherosclerosis-prone areas

Lack of pFN significantly reduced the size and number of atherosclerotic lesions. It has been postulated and confirmed in this study (Fig 1B) that FN is deposited at atherosclerosis-prone areas before lesions become visible (Hahn et al, 2009; Orr et al, 2005). To this end, we treated ApoE$^{-/-}$FN$^{fl/fl}$, ApoE$^{-/-}$FN^{VavCre} and ApoE$^{-/-}$FN^{MxCre} mice for 1 week with a high-fat diet and subsequently compared the extent of FN depositions in cross-sections of the atherosclerosis-prone lesser curvature of aortic arches.

Neither mouse strain showed evidence of atherosclerotic plaques after 1 week of high-fat diet. ApoE$^{-/-}$FN$^{fl/fl}$ and ApoE$^{-/-}$FN^{VavCre} mice showed continuous FN deposits at atherosclerosis-prone areas (Fig 4A). In contrast, ApoE$^{-/-}$FN^{MxCre} mice displayed significantly less and often

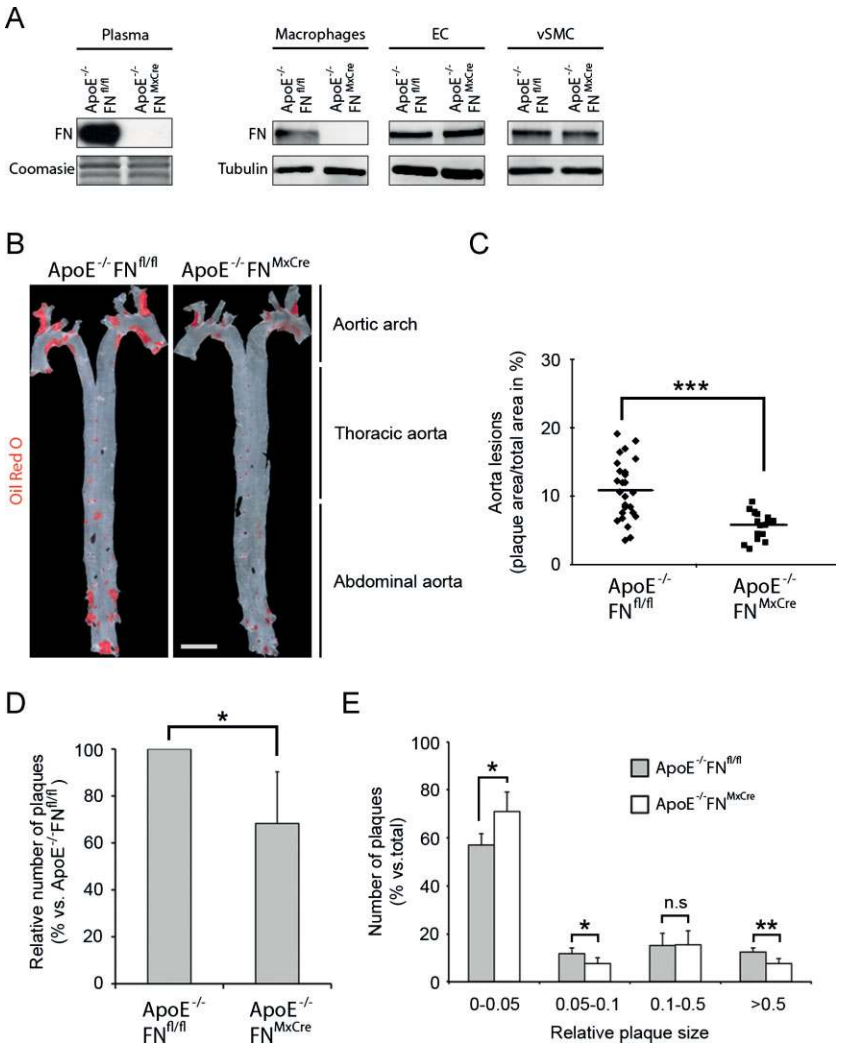

Figure 2. Reduced incidence of atherosclerosis in ApoE$^{-/-}$FN^{MxCre} mice.

A. FN levels in macrophage, EC and vSMC lysates and plasma from ApoE$^{-/-}$FN$^{fl/fl}$ and ApoE$^{-/-}$FN^{MxCre} mice, respectively. Tubulin levels served as loading control.

B. Whole-mount of longitudinally opened aortas from ApoE$^{-/-}$FN$^{fl/fl}$ and ApoE$^{-/-}$FN^{MxCre} mice stained with Oil Red O after 12 weeks on a high-fat diet. Scale bar represents 0.5 cm.

C. Quantification of atherosclerotic lesions in aortas from ApoE$^{-/-}$FN$^{fl/fl}$ ($n = 26$) and ApoE$^{-/-}$FN^{MxCre} ($n = 18$) mice after 12 weeks on a high-fat diet. Data is presented as a mean of atherosclerotic plaque area per total aorta area. Values are mean ± SD; $p = 0.000007$. n.s. = not significant.

D. Quantification of plaque number per aorta. Data is presented as mean of number of plaques per aorta from ApoE$^{-/-}$FN$^{fl/fl}$ ($n = 26$) and ApoE$^{-/-}$FN^{MxCre} ($n = 18$) mice. Values are percentage ± SD; $^{*}p = 0.03$.

E. Quantification of relative size of single lesions. Values are mean ± SD; $p = 0.024$, 0.035, 0.49 and 0.0014. n.s. = not significant.

discontinuous FN staining at the corresponding sites (Fig 4A). These results indicate that pFN, but not haematopoietic cell-derived FN, is deposited at atherosclerosis-prone sites prior to the development of atherosclerotic lesions.

Obesity and hypercholesterolemia are major risk factors for developing atherosclerosis (Lusis, 2000). Since hepatocytes play an important role in cholesterol homeostasis and FN is deleted in these cells, we determined total cholesterol, high-density lipoprotein (HDL) cholesterol and glucose levels and body weight in ApoE$^{-/-}$FN$^{fl/fl}$ and ApoE$^{-/-}$FN^{MxCre} mice treated for 12 weeks with a high-fat diet. We found no differences in either cholesterol, HDL (Fig 4B) and glucose levels (Fig 4C) or in body weight (Fig 4D) between ApoE$^{-/-}$FN$^{fl/fl}$ and ApoE$^{-/-}$FN^{MxCre} mice. These results exclude an involvement of risk factors in the differential development of atherosclerosis in ApoE$^{-/-}$FN$^{fl/fl}$ and ApoE$^{-/-}$FN^{MxCre} mice.

Expression of inflammatory mediators and recruitment of monocytes are reduced in ApoE$^{-/-}$FN^{MxCre} mice

Integrin-FN interactions are believed to promote monocyte/macrophage recruitment and to maintain an inflammatory milieu at atherosclerosis-prone sites by sustaining shear stress-induced NF-κB and PAK activation in ECs, which in turn leads to the expression of downstream genes such as ICAM-1 (Orr et al, 2007) or the activation of signalling molecules such as JNK (Hahn et al, 2009). To analyze whether pFN modulates NF-κB, PAK and JNK activity *in vivo*, we compared the levels of the phosphorylated NF-κB subunit p65, phospho-PAK, phospho-JNK and ICAM-1 on cross-sections of the atherosclerosis-prone lesser curvatures of aortic arches from ApoE$^{-/-}$FN$^{fl/fl}$ and ApoE$^{-/-}$FN^{MxCre} mice fed for 1 week with a high-fat diet. ApoE$^{-/-}$FN$^{fl/fl}$ mice had abundant phospho-NF-κB/p65, phospho-PAK throughout ECs, phospho-JNK enriched in nuclei and ICAM-1 on the luminal surface of the ECs (Fig 5A). In contrast, ApoE$^{-/-}$FN^{MxCre} mice displayed lower levels of phospho-NF-κBp65, phospho-PAK, phospho-JNK and ICAM-1 in corresponding areas (Fig 5A). Interestingly, atherosclerotic plaques of ApoE$^{-/-}$FN$^{fl/fl}$ and ApoE$^{-/-}$FN^{MxCre} mice fed for 10 weeks with a high-fat diet showed similar expression of all tested inflammatory markers (Supporting Information Fig 2A). These results indicate that depositions of pFN facilitate activation of inflammatory mediators at atherosclerosis-prone sites *in vivo*.

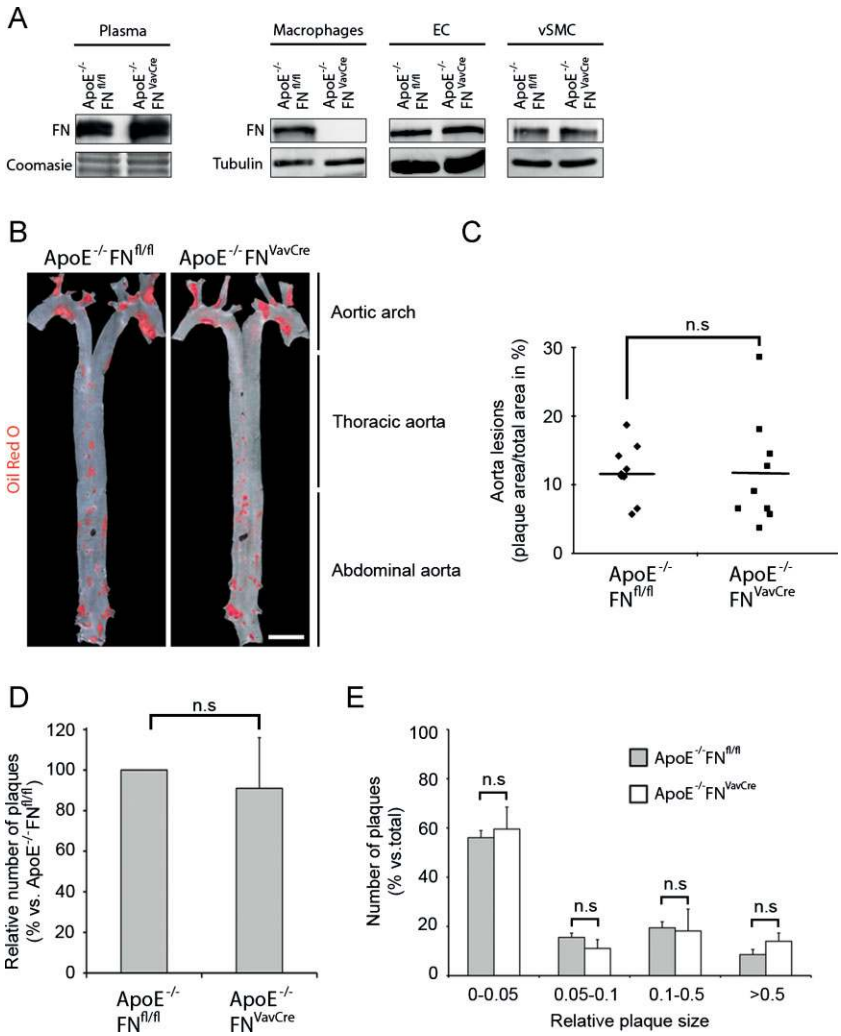

Figure 3. Normal incidence of atherosclerosis in ApoE$^{-/-}$FN^{VavCre} mice.

A. FN levels in macrophage, EC and vSMC lysates and plasma from ApoE$^{-/-}$FN$^{fl/fl}$ and ApoE$^{-/-}$FN^{VavCre} mice, respectively. Tubulin levels served as loading control.

B. Whole-mount of longitudinally opened aortas from ApoE$^{-/-}$FN$^{fl/fl}$ and ApoE$^{-/-}$FN^{VavCre} mice stained with Oil Red O after 12 weeks on a high-fat diet. Scale bar represents 0.5 cm.

C. Quantification of atherosclerotic lesions in aortas from ApoE$^{-/-}$FN$^{fl/fl}$ ($n = 9$) and ApoE$^{-/-}$FN^{VavCre} ($n = 9$) mice after 12 weeks on a high-fat diet. Data is presented as a mean of atherosclerotic plaque area per total aorta area. Values are mean ± SD; $p = 0.96$. n.s. = not significant.

D. Quantification of plaque numbers per aorta. Data is presented as mean of number of plaques per aorta from ApoE$^{-/-}$FN$^{fl/fl}$ ($n = 9$) and ApoE$^{-/-}$FN^{VavCre} ($n = 9$) mice. Values are percentage ± SD; $p = 0.78$. n.s. = not significant.

E. Quantification of the relative size of single lesions. Values are mean ± SD; $p = 0.27$, 0.08, 0.41 and 0.055. n.s. = not significant.

To further confirm these results, we cultured ECs in the presence and absence of pFN and monitored the expression of ICAM-1 by WB. In line with our *in vivo* results, ICAM-1 levels were reduced in ECs when they were cultured in the absence of pFN (Fig 5B).

Adhesion of monocytes to the endothelium is required for the initiation of atherosclerosis (Woollard & Geissmann, 2010). To analyze whether pFN depositions modulate adhesion of monocytes to ECs, we analyzed leukocyte adhesion on the endothelium in atherosclerosis-prone regions of the carotid artery of ApoE$^{-/-}$FN$^{fl/fl}$ and ApoE$^{-/-}$FN^{MxCre} mice using intravital microscopy and found that the number of adherent leukocytes was reduced in ApoE$^{-/-}$FN^{MxCre} mice when compared to ApoE$^{-/-}$FN$^{fl/fl}$ control littermates (Fig 5C and D). Since the number of circulating leukocytes is influencing their adhesion to the endothelium, we determined their numbers and found that they were similar in ApoE$^{-/-}$FN$^{fl/fl}$ and ApoE$^{-/-}$FN^{MxCre} mice (unpublished observation). The adhesion of leukocytes to the endothelium is mediated by the interaction of α4β1 integrins to VCAM-1 (Barringhaus et al, 2004). Immunostaining of cross-sections of aortic arches with anti-VCAM-1 antibodies and FACS analyses of leukocytes to quantify α4β1 integrin surface levels revealed normal levels of both adhesion molecules in ApoE$^{-/-}$FN$^{fl/fl}$ and ApoE$^{-/-}$FN^{MxCre} mice fed for 1 week with a high-fat diet (Supporting Information Fig 2B and 2C).

Next, we measured cell adhesion of Mac-1-positive cells to monolayers of ECs under static and laminar flow conditions, both in the presence and absence of pFN. We used bEnd5 endothelioma cells to test adhesion, since they were shown to promote adhesion of haematopoietic cells equally well as primary ECs (Steiner et al, 2010). Mac-1-positive cells cultured in absence of pFN were suspended in pFN-free medium or pFN-complemented medium (10 μg/ml) and then seeded onto a bEnd5 monolayer. Quantification of adherent cells revealed that twofold more Mac-1-positive cells adhered to the bEnd5 monolayer when they were cultured in pFN-complemented medium as compared to pFN-free medium (Fig 5E), indicating that soluble pFN promotes adhesion of Mac-1-positive cells to ECs.

During atherosclerosis, low-density lipoprotein (LDL) particles aggregate and become oxidized in the vascular ECM. Oxidized LDL will be taken up by macrophages resulting in the

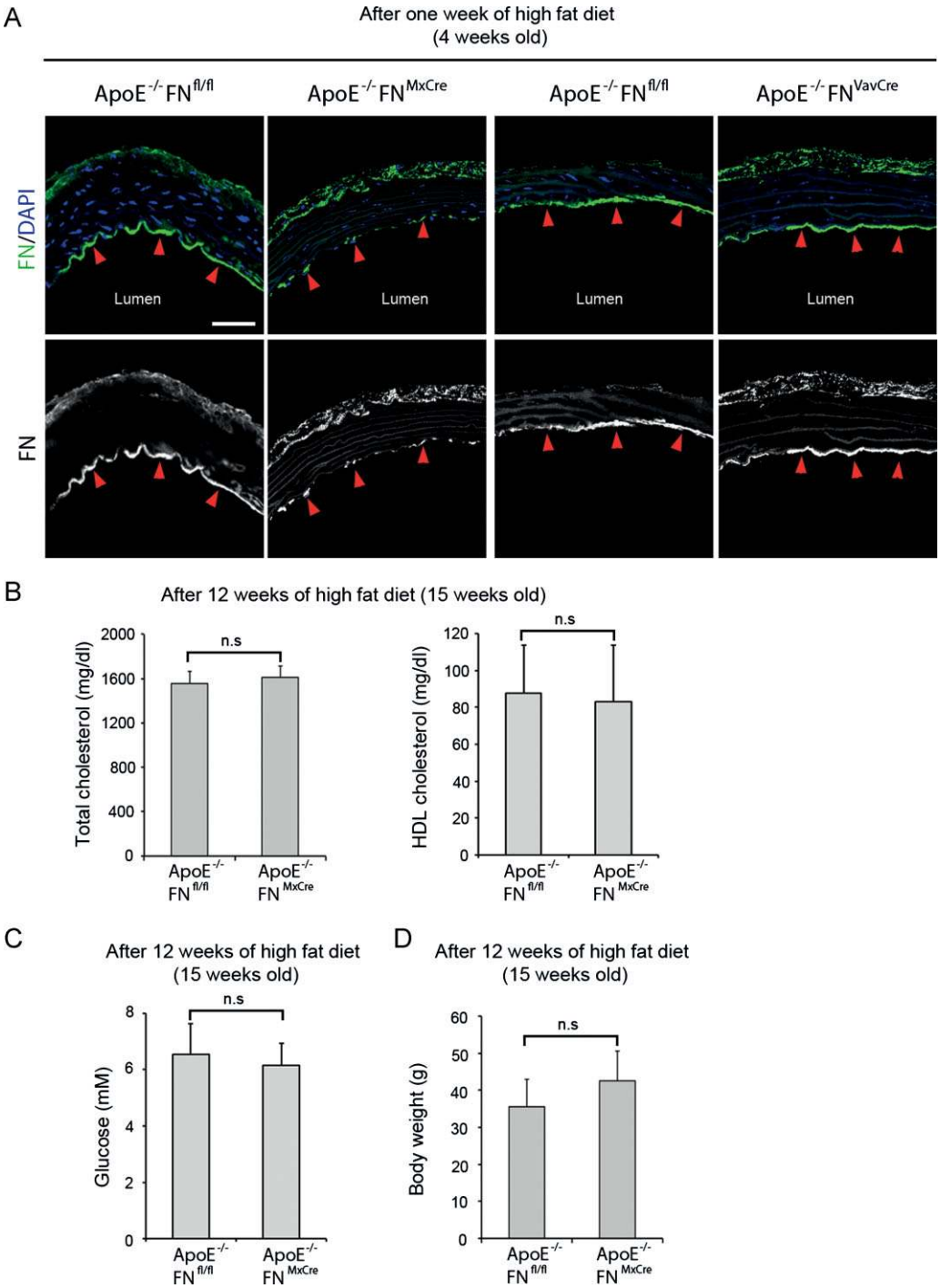

Figure 4. Reduced FN depositions in the aortic arch of ApoE$^{-/-}$FN^{MxCre} mice.

A. Immunostaining of FN in the lesser curvature of the aortic arch from ApoE$^{-/-}$FN^{MxCre}, ApoE$^{-/-}$FN^{VavCre} mice and their respective ApoE$^{-/-}$FN$^{fl/fl}$ mice. Arrowheads point to FN signals at the luminal side of the arch. Nuclei are visualized with DAPI. Scale bar represents 75 μm in all images.

B. Fasting cholesterol and HDL cholesterol levels of ApoE$^{-/-}$FN$^{fl/fl}$ ($n = 13$) and ApoE$^{-/-}$FN^{MxCre} ($n = 13$) mice after 12 weeks on a high-fat diet. Values are mean ± SD; $p = 0.33$. n.s. = not significant.

C. Fasting glucose levels of ApoE$^{-/-}$FN$^{fl/fl}$ ($n = 13$) and ApoE$^{-/-}$FN^{MxCre} ($n = 13$) mice after 12 weeks on a high-fat diet. Values are mean ± SD; $p = 0.15$. n.s. = not significant.

D. Body weight of ApoE$^{-/-}$FN$^{fl/fl}$ ($n = 28$) and ApoE$^{-/-}$FN^{MxCre} ($n = 16$) mice after 12 weeks on a high fat-diet. Values are mean ± SD; $p = 0.11$. n.s. = not significant.

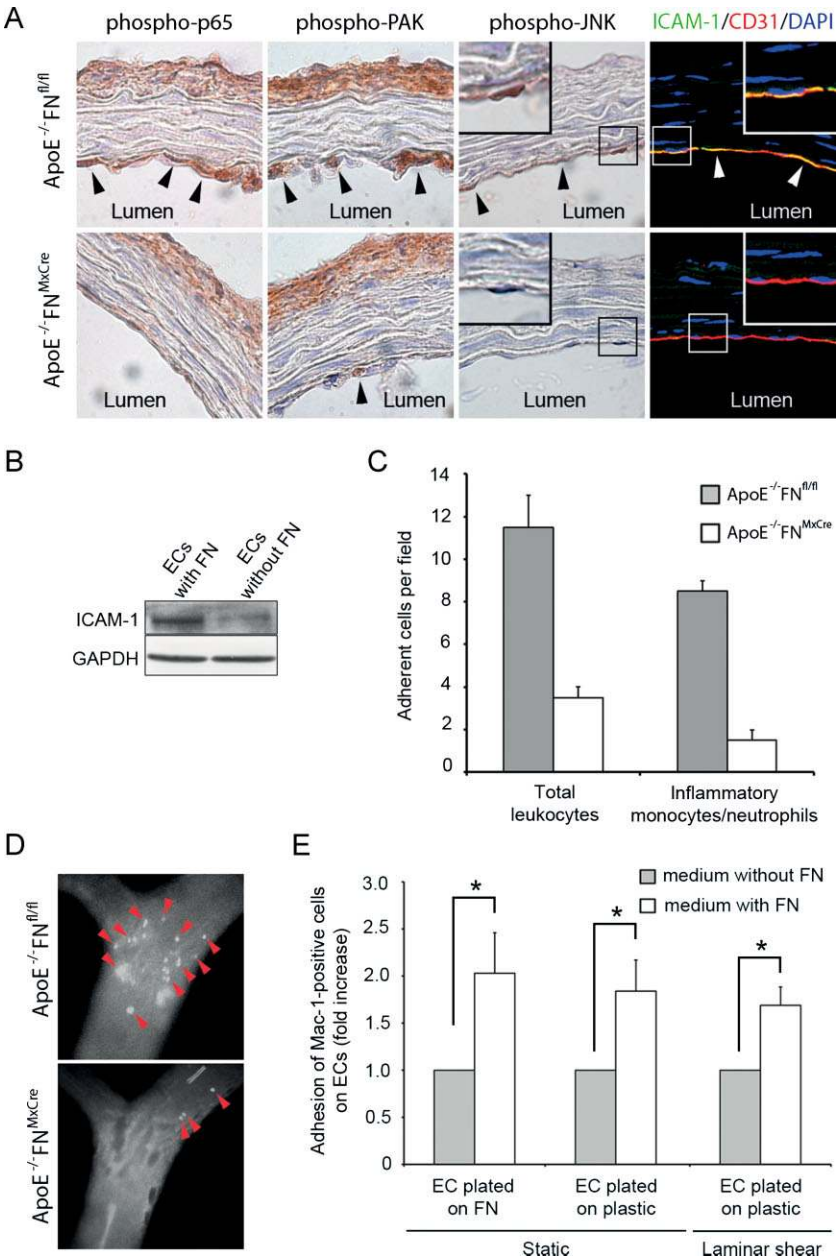

Figure 5. Reduced NF-κB and PAK activation and macrophage recruitment into atheroprone areas of ApoE$^{-/-}$FN^{MxCre} mice.

A. Immunostaining of phosho-NFκB/p65, phospho-PAK, phospho-JNK and ICAM-1 in the lesser curvature of the aortic arch from ApoE$^{-/-}$FN$^{fl/fl}$ and ApoE$^{-/-}$FN^{MxCre} mice. Arrowheads point to immunosignals in ECs.

B. Western blot for ICAM-1 in lysates from ECs cultured for 36 h in the presence or absence of pFN.

C. Adhesion of leukocytes and inflammatory monocytes/neutrophils to carotid arteries of ApoE$^{-/-}$FN$^{fl/fl}$ and ApoE$^{-/-}$FN^{MxCre} mice fed with high-fat diet for 4.5 weeks. Values are mean ± SD.

D. Representative images of inflammatory monocytes/neutrophils adhering (arrowheads) to the luminal side of the external carotid artery in ApoE$^{-/-}$FN$^{fl/fl}$ and ApoE$^{-/-}$FN^{MxCre} mice.

E. Quantification of adhesion of Mac-1-positive cells on a monolayer of ECs under static condition and laminar shear (2.5 dyne/cm^2). Values are mean ± SD and normalized to adherent cells in the presence of FN in the culture medium; $p = 0.025$, 0.023 and 0.029.

formation of aggregated and oxidized LDL foam cells (Woollard & Geissmann, 2010). To test whether pFN modulates lipid accumulation in plaques, we stained cross-sections of atherosclerotic plaques from ApoE$^{-/-}$FN$^{fl/fl}$ and ApoE$^{-/-}$FN^{MxCre} mice with Oil Red O. Lipids were detected in the core region of the plaques and a similar lipid accumulation was found in ApoE$^{-/-}$FN$^{fl/fl}$ and ApoE$^{-/-}$FN^{MxCre} mice (Fig 6A).

To determine whether FN affects macrophage uptake of modified LDL, we incubated freshly isolated macrophages from ApoE$^{-/-}$FN$^{fl/fl}$ and ApoE$^{-/-}$FN^{MxCre} mice (Supporting Information Fig 3) with LDL and acLDL and then stained them with Oil Red O. The intracellular lipid accumulation was similar in macrophages from ApoE$^{-/-}$FN$^{fl/fl}$ and ApoE$^{-/-}$FN^{MxCre} mice (Fig 6B). Finally, we quantified the acLDL uptake by macrophages from ApoE$^{-/-}$FN$^{fl/fl}$ and ApoE$^{-/-}$FN^{MxCre} mice after incubating them for 4 and 24 h with acLDL and found that also the acLDL uptake was normal (Fig 6C). Collectively, these results indicate that FN is dispensable for foam cell formation.

Atherosclerotic lesions in ApoE$^{-/-}$FN^{MxCre} mice lack the fibrous cap

Advanced atherosclerotic lesions are characterized by a subendothelial accumulation of vSMCs, which synthesize and deposit a collagen- and FN-rich matrix into the fibrous cap (Newby & Zaltsman, 1999). To test whether loss of pFN alters fibrous cap formation, we immunostained cross-sections of similarly sized atherosclerotic plaques from ApoE$^{-/-}$FN$^{fl/fl}$ and ApoE$^{-/-}$FN^{MxCre} mice for Mac-1 to visualize monocyte/

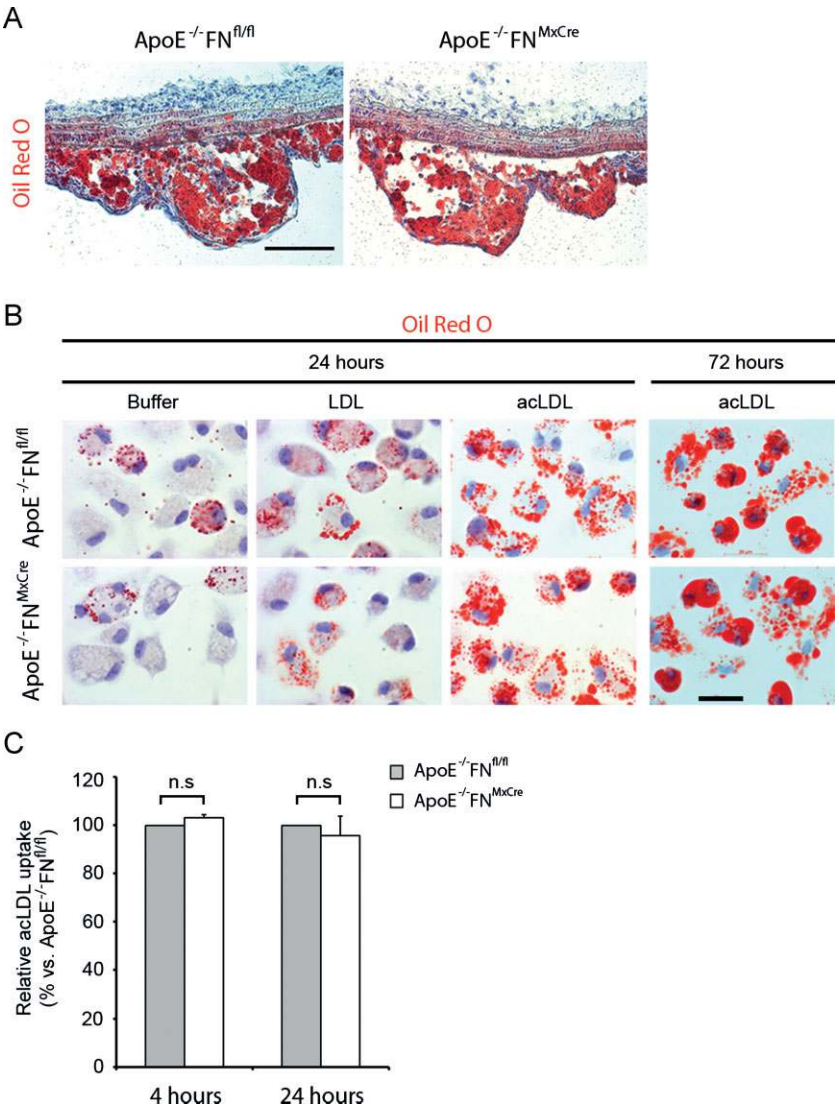

Figure 6. Normal foam cell formation in ApoE$^{-/-}$FN^{MxCre} mice.

A. Staining atherosclerotic plaques from ApoE$^{-/-}$FN$^{fl/fl}$ and ApoE$^{-/-}$FN^{MxCre} mice 12 weeks after a high fat diet with Oil Red O and haematoxylin. Scale bar represents 100 μm.

B. Staining of macrophages from ApoE$^{-/-}$FN$^{fl/fl}$ and ApoE$^{-/-}$FN^{MxCre} mice with Oil Red O and haematoxylin 24-h after incubating them with LDL or AcLDL, respectively. Scale bar represents 20 μm.

C. Quantification of acLDL uptake by macrophages from ApoE$^{-/-}$FN$^{fl/fl}$ and ApoE$^{-/-}$FN^{MxCre} mice. Values are mean ± SD; $p = 0.36$ and 0.29. n.s. = not significant.

macrophages, Thy-1.2/CD3 to visualize T cells, alpha-smooth muscle actin (αSMA) to visualize vSMCs and the ECM proteins FN and collagen type I (Col-I). After 12 weeks of high-fat diet, atherosclerotic plaques from ApoE$^{-/-}$FN$^{fl/fl}$ mice consisted of macrophage-derived foam cells that were covered at the luminal side with a FN- and collagen-rich matrix and a continuous layer of vSMCs (Fig 7A and B and Supporting Information Fig 4A). A few T cells were detected, mainly at the edges of a few plaques (Supporting Information Fig 4B). In sharp contrast, atherosclerotic plaques from ApoE$^{-/-}$FN^{MxCre} mice lacked vSMCs and a collagen matrix and consisted mainly of macrophage-derived foam cells (Fig 7 A and B and Supporting Information Fig 4A). Similarly, atherosclerotic plaques of ApoE$^{-/-}$FN^{MxCre} mice fed for 6 months with a high-fat diet also lacked vSMCs and a collagen matrix. Distribution and number of T cells were unaffected in ApoE$^{-/-}$FN^{MxCre} mice (Supporting Information Fig 4B).

To determine whether monocyte/macrophage-derived FN contributes to vSMCs recruitment and fibrous cap formation, we analyzed lesions from ApoE$^{-/-}$FN^{VavCre} mice and found that the cellular composition of their lesions and the FN deposits in their fibrous caps were similar to ApoE$^{-/-}$FN$^{fl/fl}$ control littermates (Supporting Information Fig 4C). Together, these results indicate that pFN plays an important role in promoting the formation of the fibrous cap.

pFN stimulates vSMC migration

Why do vSMCs fail to colonize the fibrous caps in ApoE$^{-/-}$FN^{MxCre} mice? Successful accumulation of vSMCs in atherosclerotic lesions and subsequent formation of the fibrous cap depends on a number of factors including vSMC proliferation and survival rates as well as their ability to migrate into the lesions (Newby & Zaltsman, 1999). We found no apparent defects in vSMCs proliferation nor did we observe increased apoptosis in lesions from ApoE$^{-/-}$FN^{MxCre} mice subjected to high-fat diet. To test whether pFN modulates migration of vSMCs, we isolated primary vSMCs and performed chemotaxis assays using transwell motility chambers using pFN as a

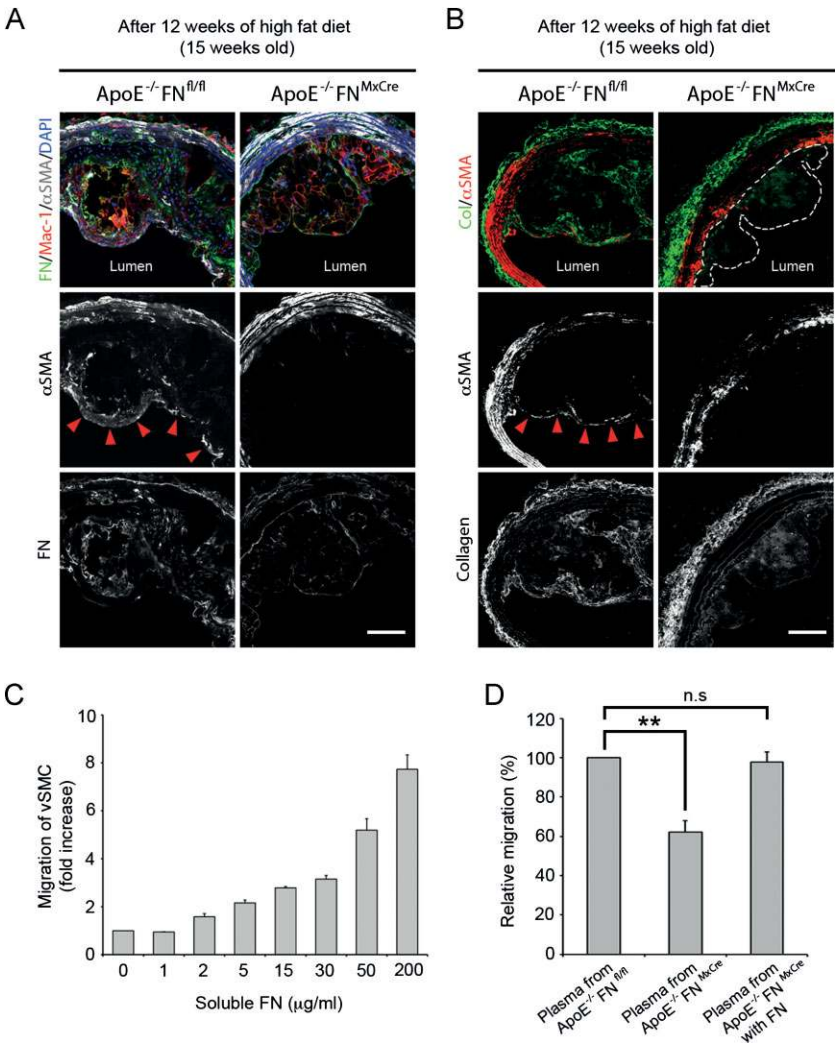

Figure 7. Atherosclerotic lesions from ApoE$^{-/-}$FN^{MxCre} mice lack fibrous caps.

A. Immunostaining of atherosclerotic plaques from ApoE$^{-/-}$FN$^{fl/fl}$ and ApoE$^{-/-}$FN^{MxCre} mice after 12 weeks of high fat diet for FN, macrophage antigen-1 (Mac-1) and αSMA. Arrowheads point to αSMA immunosignals in the fibrous cap. Nuclei are visualized with DAPI. Scale bar represents 75 μm.

B. Immunostaining of atherosclerotic plaques from ApoE$^{-/-}$FN$^{fl/fl}$ and ApoE$^{-/-}$FN^{MxCre} mice after 12 weeks of high fat diet with antibodies against collagen I and αSMA. White dotted line displays plaque surface. αSMA stains the luminal side (arrowheads). Nuclei are visualized with DAPI. Scale bar represents 75 μm.

C. Quantification of vSMC migration against FN in the lower part of Transwell chambers. Control medium lacking FN (0) was used to assess baseline migration.

D. Quantification of vSMC migration against plasma from ApoE$^{-/-}$FN$^{fl/fl}$, ApoE$^{-/-}$FN^{MxCre} mice with and without supplementation of FN (12 μg/ml). Values are percentage of migrating cells ± SD; $p = 0.0045$ and 0.1. n.s. = not significant.

chemoattractant in the lower part of the chambers. We observed that pFN increased the migration of vSMCs in a concentration-dependent manner (Fig 7C). When we added plasma samples from ApoE$^{-/-}$FN$^{fl/fl}$ and ApoE$^{-/-}$FN^{MxCre} mice to the lower part of the migration chamber, we found that plasma from ApoE$^{-/-}$FN$^{fl/fl}$ mice induced twofold higher migration rates of vSMCs than plasma from ApoE$^{-/-}$FN^{MxCre} mice (Fig 7D). Importantly, the decreased migration rates of vSMCs towards plasma derived from ApoE$^{-/-}$FN^{MxCre} mice could be rescued by supplementing the plasma with FN (Fig 7D). These results clearly indicate that pFN is a motility factor for vSMCs.

DISCUSSION

FN deposits and atherosclerotic lesions preferentially form at sites of disturbed blood flow (Hahn & Schwartz, 2009). *In vitro* studies with shear-stressed ECs cultured on FN suggest that the FN deposits enforce and maintain a pro-atherogenic milieu through integrin binding and signalling (Feaver et al, 2010). It is not known, however, whether FN serves a similar function *in vivo* and whether the FN depositions are derived from the circulation or from infiltrating monocytes and/or resident ECs. To address these questions, we generated mice lacking the *FN* gene either in hepatocytes and/or haematopoietic cells and crossed them with atherosclerosis-prone ApoE-null mice and fed them a high-fat diet. Loss of FN expression in blood cells modulated neither the development nor progression of atherosclerosis in mice. In contrast, loss of pFN abrogated FN depositions at atherosclerosis-prone sites resulting in the formation of smaller and fewer atherosclerotic lesions. However, they were covered only with a thin layer of matrix proteins, which is usually a sign of fragility and increased susceptibility for ruptures in human atherosclerotic plaques. These findings suggest a dual function for pFN during atherosclerosis: it supports plaque initiation by providing an adhesive matrix for monocytes and at late stages, it protects the lesions by controlling the formation of the fibrous cap. Thus, targeting atheroma initiation and growth by modulating FN production might have the unforeseen consequences of promoting plaque rupture and arterial occlusions resulting in a significant increase in vascular morbidity and mortality.

The subendothelial matrix of the healthy vasculature is mainly composed of basement membrane (BM) components including collagen IV and laminins. During pathological situations such as inflammation, wound healing or atherosclerosis transitional matrix proteins such as FN or fibrinogen are deposited into the subendothelial matrix (Hahn & Schwartz, 2009). In atherosclerosis, FN is deposited at sites of disturbed flow before fatty streaks are formed (Hahn & Schwartz, 2009; Hahn et al, 2009; Orr et al, 2005) but the source of the FN deposits is not known. *In vitro* studies have shown that disturbed flow induces the expression and deposition of FN by ECs (Feaver et al, 2010) suggesting that shear-stressed ECs deposit FN into the vessel wall. We confirmed these findings showing that FN is indeed deposited into the subendothelial space at sites of disturbed blood flow. Since pFN can be transferred from the plasma into tissues (Moretti et al, 2007; Oh et al, 1981), we next tested whether pFN contributes to the FN depositions. To this end, we ablated a conditional *FN*-null allele in ApoE-null mice with the *Mx-Cre* transgene ($ApoE^{-/-}FN^{MxCre}$) that deletes efficiently in hepatocytes and haematopoietic cells, and fed the offspring a high fat diet. The *Mx-Cre* transgene can also delete genes at low efficiency in other tissues than liver and blood cells, which is, however, efficiently compensated by diffusion of FN from non-deleted neighbouring cells (Sakai et al, 2001). The $ApoE^{-/-}FN^{MxCre}$ offspring showed very little FN at atheroprone areas suggesting that pFN represents a major source for FN depositions at the atherosclerosis-prone areas of the vasculature. The presence of residual FN in vessel walls of $ApoE^{-/-}FN^{MxCre}$ mice indicates that small contributions from ECs and/or vSMCs may add to the FN depositions at atherosclerosis-prone areas. Previous reports associating increased pFN levels with atherosclerosis (Orem et al, 2003) and ischemic heart disease (Ozcelik et al, 2009; Song et al, 2001; Taznatos et al, 2009) support a role of pFN as atherosclerosis promoting factor. On the other hand, however, it has also been shown that pFN levels were unchanged or even decreased in cohorts of atherosclerosis patients (Vavalle et al, 2007; Zhang et al, 2006). It is thus possible that other risk factors, which probably depend on the patient population, are able to either attenuate or aggravate the effect of pFN on the course of atherosclerosis. Unfortunately, the nature of these risk factors is not known.

In atherosclerosis, it is believed that binding of fibrillar collagens to α2β1 prevents pro-inflammatory signals, while FN sustains a shear-stressed induced inflammatory environment and therefore is thought to aggravate the course of the disease. Mechanistically, FN mediates its pro-inflammatory role through β1-containing integrins, most likely α5β1 (Orr et al, 2006), which in turn induces phosphorylation of NF-κB through the activation of the small GTPase Rac1 (Tzima et al, 2002). In line with these findings we found that ECs of $ApoE^{-/-}FN^{MxCre}$ mice contain significantly less of the phosphorylated NF-κB subunit p65 and less phosphorylated PAK, and develop smaller plaques than control mice. In line with reduced NF-κB activity we also observed reduced expression of the downstream gene *ICAM-1* on ECs. Consequently, the adhesion of monocytes to the endothelium at atherosclerosis-prone regions in $ApoE^{-/-}FN^{MxCre}$ mice was also reduced when compared to control littermates, providing a good explanation for the reduced recruitment of monocytes to atherosclerosis-prone sites. Interestingly, we found that the levels of inflammatory markers in developed lesions of $ApoE^{-/-}FN^{MxCre}$ mice were comparable with those of control mice, indicating that pFN is required for inflammation during plaque initiation, but not anymore once the plaques have formed. Since the deletion of the *FN* gene in monocytes by Vav-Cre did not affect the course of atherosclerosis, we expected normal monocyte recruitment to plaques in these mice, although we did not confirm this by intravital microscopy. In summary, we collected several lines of evidence suggesting that monocyte recruitment is indeed impaired in pFN-deficient mice: the expression of ICAM-1 on ECs was markedly reduced, the adhesion of monocytes to the endothelium was reduced in pFN-deficient mice, and the number and size of atherosclerotic plaques was significantly diminished in $ApoE^{-/-}FN^{MxCre}$ mice.

The reduced number and size of atherosclerotic plaques in $ApoE^{-/-}FN^{MxCre}$ mice corroborate previous observations made using *in vitro* systems. In addition, our findings revealed a previously unknown function for FN in atherosclerosis. Almost all atherosclerotic lesions in $ApoE^{-/-}FN^{MxCre}$ mice were devoid of vSMC, contained reduced levels of collagen I and lacked a fibrous cap, which points to a role for FN in the reinforcement of atherosclerotic plaques. Atherosclerotic plaques that are not stabilized with fibrous caps in humans lead to an increased likelihood of rupture and subsequent thrombus-mediated vascular occlusion leading to myocardial infarction, stroke and sudden death (Lusis, 2000). Unfortunately, plaque ruptures with thrombosis do not occur in mouse models and therefore, the consequences could not be tested (Glass & Witztum, 2001; Libby et al, 2011). The formation of a fibrous cap critically depends on the activation and proliferation of vSMCs in the intima of the affected vessel and their subsequent migration into the plaque area where they deposit a collagen-rich matrix. Since we found normal proliferation and survival rates of vSMCs in $ApoE^{-/-}FN^{MxCre}$ mice, we conclude that the vascular FN deposits represent a trigger for the recruitment of vSMCs. This notion is supported by our *in vitro* experiments demonstrating that vSMCs were less efficient at migrating towards plasma lacking pFN.

These new findings strongly argue against the use of inhibitors designed to treat atherosclerosis by blocking the function of FN, such as by using peptides derived from FN. This type of treatment would inhibit pro-inflammatory signalling and thus reduce the number and size of atherosclerotic plaques but would also at the same time destabilize these plaques and increase the danger of thrombus formation and thrombotic diseases. Furthermore, reducing pFN levels would also destabilize thrombi and trigger the shedding of platelet clumps into the circulation (Ni et al, 2003) resulting in chronic embolism.

MATERIALS AND METHODS

Animal procedures

$ApoE^{-/-}$ (Jackson Laboratory) and $FN^{fl/fl}$ mice (Sakai et al, 2001) were intercrossed with Mx-Cre transgenic mice (Kuhn et al, 1995; Schneider

The paper explained

PROBLEM:

Vascular occlusion of atheromatous arteries is the commonest cause of death in the western world. The main cause of vascular occlusions is the rupture of atherosclerotic plaques followed by thrombus formation. Atherosclerotic plaques are asymmetric focal thickenings of the artery consisting of lipids, various cell types and ECM including FN. Expression of FN is elevated in vessel walls of atherosclerotic regions, however, the source and functions of FN in atherosclerosis are not clear.

RESULTS:

In our study, we show that atherosclerosis-prone mice lacking hepatocyte-derived pFN and fed with a pro-atherogenic diet lack FN deposits and show reduced pro-inflammatory signals at atherosclerosis-prone areas resulting in significantly smaller and fewer atherosclerotic plaques. Unexpectedly, the atherosclerotic lesions were devoid of fibrous caps, which play an important role for plaque stability and to prevent plaque rupture.

IMPACT:

Our results demonstrate that FN plays a dichotomous role in atherosclerosis: while FN worsens the course of atherosclerosis by increasing the atherogenic plaque area, it stabilizes the plaques with fibrous caps and protects from secondary damage and vascular occlusion.

et al, 2003) to produce ApoE$^{-/-}$FN^{MxCre} mice, or with Vav-Cre transgenic mice (Georgiades et al, 2002) to produce ApoE$^{-/-}$FN^{VavCre} mice. Deletion of the floxed *FN* alleles was induced in 2-week-old mice by a single intraperitoneal injection of 175 μg poly-IC (Sigma).
Atherosclerosis was accelerated by feeding the mice for 12 weeks with a high fat diet (provided by Altromin, Lage/Lippe, Germany) containing 21% fat, 0.15% cholesterol but lacking cholate (composition according to Harlan Teklad TD88137 diet). All experiments with mice were performed in accordance to German guidelines and regulations.

Atherosclerotic lesion analysis

Mice were anesthetized with Avertin, hearts were perfused with 15 ml of phosphate-buffered saline (PBS) containing 5 mM ethylenediaminetetracetic acid (EDTA) and then with PBS containing 2% paraformaldehyde (PFA), 7.5% sucrose. The adventitia was thoroughly cleaned under a dissecting microscope, and the aorta was cut open longitudinally and pinned on to a silicone plate. After 5 min equilibration in 60% isopropanol, aortas were stained with Oil Red O (Sigma, Germany), plaques were analyzed under the Leica MZ16FA stereomicroscope, and quantified with Metamorph® software. The aortic lesions of each animal are presented as percentage of the total aortic luminal surface area.

Plasma cholesterol

Total and HDL cholesterol levels in plasma were quantified as previously described (Dunér et al, 2011; Fredrikson et al, 2003).

Plasma glucose measurement

Plasma glucose was measured using a commercial kit (Abcam).

Antibodies

The following antibodies were used: biotinylated rat anti-Mac-1 monoclonal antibody (Pharmingen), CD3-PE, Thy-1.2 CD90.2, GM-130, ICAM-1, PECAM-1 (CD31) (all from Pharmingen), Cy3-coupled mouse anti-αSMA antibody (Sigma), rabbit anti-FN polyclonal antibody (Millipore), rabbit anti-Col-I antibody (Millipore), phospho-NFκB p65 (Santa Cruz), phospho-PAK1/2 (Cell Signaling), phosphor-JNK (Cell Signaling). Secondary antibodies were purchased from Jackson Immuno Research Laboratories, Molecular Probes or Invitrogen.

Histology and immunostaining

Heart and aorta tissues were embedded into a cryo-matrix (Thermo) and 10 or 12 μm sections were prepared using a cryotome. Sections were blocked with 3% bovine serum albumin (BSA) 0.2% Triton-X in PBS and incubated with antibodies.

Intravital microscopy

Intravital microscopy of the left carotid artery was performed as described previously (Drechsler et al, 2010). The left jugular vein was cannulated with polyethylene tubing (PE50) for the intravenous administration of anti-Gr1 antibodies (RB6-8C5, 2.5 μg/mouse) for visualizing inflammatory monocytes and neutrophils and rhodamine 6G to visualize total leukocytes. Intravital microscopy was performed with an Olympus BX51 microscope equipped with a Hamamatsu 9100-02 EMCCD camera and a 10× saline-immersion objective. For image acquisition and analysis Olympus cell^{R} software was used.

Isolation of smooth muscle cells

Aortas were dissected, longitudinally opened, washed with PBS, cut and digested with digestion buffer (2 mg/ml collagenase type II and 0.5 mg/ml elastase in Dulbecco's modified Eagle medium (DMEM)) for 30 min at 37°C. Digestion was terminated with 10% foetal bovine serum (FBS) in DMEM. Released cells were centrifuged and re-suspended in DMEM containing 10% FBS, transferred to 6-well dishes and further expanded for analysis.

Isolation of aortic endothelial cells

Cells were isolated as previously described (Kobayashi et al, 2005).

In vitro foam cell formation assay

Thioglycolate-elicited peritoneal macrophages were plated on 12-well plates in macrophage serum-free medium (Macrophage-SFM, Invitrogen). After 24 h, non-adherent cells were washed off, and macro-

phages were incubated in fresh serum-free medium complemented with 50 μg/ml native, acetylated human LDL (acLDL) or buffer control for 24–72 h. Cells were stained for 60 min with Oil Red O and counterstained with haematoxylin.

Modified LDL uptake

Thioglycolate-elicited peritoneal macrophages were plated on coverslips in macrophage serum-free medium (Invitrogen). After 24 h, non-adherent cells were washed off and adherent macrophages were incubated in serum-free medium complemented with 10 μg/ml native, acLDL:Dil for 4 or 24 h. Afterwards cells were washed with PBS, fixed with 4% PFA and nuclei were stained with 4,6-diamidino-2-phenylindole (DAPI). Fluorescence was analyzed with ImageJ software. Five microscopic fields were counted per experiment.

SDS–PAGE and immunoblotting

Plasma samples and cells were incubated in lysis buffer (150 mM NaCl, 50 mM Tris pH 7.4, 1 mM EDTA, 1% Triton X-100 supplemented with protease inhibitors (Roche)), homogenized in Laemmli sample buffer and boiled for 5 min. Proteins were resolved by SDS–polyacrylamide gel electrophoresis (SDS–PAGE) gels and then electrophoretically transferred from the gels onto nitrocellulose membranes, which were subsequently incubation with antibodies. Bound antibodies were detected using enhanced chemiluminescence (Millipore Corporation, Billerica, USA).

Migration assay

Migration assays were performed in 8 μm pore size chamber inserts (BD Falcon). 4×10^4 vSMCs were seeded into the chambers, which were then transferred into 24-well plates containing serum-free medium supplemented with dilutions of pFN or plasma from control and $ApoE^{-/-}FN^{MxCre}$ mice, respectively.

After an overnight incubation, the cells in the bottom part of the chamber were fixed in 4% PFA and stained with 0.2% crystal violet. Five microscopic fields per chamber were counted. Data are represented as percentage of reference cell number/field. Three independent experiments were performed, each of them in triplicate.

Adhesion assays

Adhesion assays of primary peritoneal macrophages to the endothelioma cell line bEnd5 were carried out as follows. bEnd5 cells were cultured in serum-free medium in 4-well NUNC chamber slides until confluence, either on 1 μg/ml FN or on plastic. Macrophages were isolated and co-cultured with bEnd5 cells for 6 h, either with additional FN (10 μg/ml) or without in the medium. Cells were washed with PBS, fixed with 4% PFA and stained for Mac-1. Six microscopic fields were counted per experiment.

Adhesion assays of primary peritoneal macrophages under flow conditions were carried out with bEnd5 cells. bEnd5 cells were cultured in serum-free medium or serum-free medium containing 10 μg/ml FN in a μ-Slide I $^{0.4}$ Luer (Ibidi) over night. Primary macrophages were isolated and cultured in FN-free medium or medium containing 10 μg/ml FN. Macrophages were perfused at 2.5 dyne/cm^2 at 37°C over the endothelial monolayer for 10 min. Cells were washed with PBS, fixed with 4% PFA, stained for the Mac-1 antigen and the adherent macrophages were then counted in 10 microscopic fields per experiment.

Statistical analysis

The statistical analysis was performed using the Student's-*t*-test. The values are presented as mean ± SD.

Author contributions

The study was conceived by RF. IR, KB, EM performed most experiments and analyzed them together with RF. EB, PD and JN made cholesterol measurements and OS intravital microscopy experiments. RF and EM wrote the manuscript. All authors read and approved the manuscript.

Acknowledgements

The authors thank MSc Klaus Kemmerich for excellent technical assistance. KB was supported by EMBO. The work was funded by the Deutsche Forschungsgemeinschaft (SFB-914; to OS and RF) and the Max Planck Society (to RF).

Supporting Information is available at EMBO Molecular Medicine online.

The authors declare that they have no conflict of interest.

References

Astrof S, Hynes RO (2009) Fibronectins in vascular morphogenesis. Angiogenesis 12: 165-175

Babaev VR, Porro F, Linton MF, Fazio S, Baralle FE, Muro AF (2008) Absence of regulated splicing of fibronectin EDA exon reduces atherosclerosis in mice. Atherosclerosis 197: 534-540

Barringhaus KG, Phillips JW, Thatte JS, Sanders JM, Czarnik AC, Bennett DK, Ley KF, Sarembock IJ (2004) Alpha4beta1 integrin (VLA-4) blockade attenuates both early and late leukocyte recruitment and neointimal growth following carotid injury in apolipoprotein E (−/−) mice. J. Vasc. Res. 3: 252-260

Drechsler M, Megens RT, van Zandvoort M, Weber C, Soehnlein O (2010) Hyperlipidemia-triggered neutrophilia promotes early atherosclerosis. Circulation 18: 1837-1845

Dunér P, To F, Beckmann K, Björkbacka H, Fredrikson GN, Nilsson J, Bengtsson E (2011) Immunization of apoE−/− mice with aldehyde-modified fibronectin inhibits the development of atherosclerosis. Cardiovasc. Res. 91: 528-536

Feaver RE, Gelfand BD, Wang C, Schwartz MA, Blackman BR (2010) Atheroprone hemodynamics regulate fibronectin deposition to create positive feedback that sustains endothelial inflammation. Circ. Res. 106: 1703-1711

Fredrikson GN, Söderberg I, Lindholm M, Dimayuga P, Chyu KY, Shah PK, Nilsson J (2003) Inhibition of atherosclerosis in apoE-null mice by immunization with apoB-100 peptide sequences. Arterioscler. Thromb. Vasc. Biol. 23: 879-884

Funk SD, Yurdagul AJr, Green JM, Jhaveri KA, Schwartz MA, Orr AW (2010) Matrix-specific protein kinase A signaling regulates p21-activated kinase activation by flow in endothelial cells. Circ. Res. 106: 1394-1403

George EL, Georges-Labouesse EN, Patel-King RS, Rayburn H, Hynes RO (1993) Defects in mesoderm, neural tube and vascular development in mouse embryos lacking fibronectin. Development 119: 1079-1091

Georgiades P, Ogilvy S, Duval H, Licence DR, Charnock-Jones DS, Smith SK, Print CG (2002) VavCre transgenic mice: a tool for mutagenesis in hematopoietic and endothelial lineages. Genesis 34: 251-256

Glass CK, Witztum JL (2001) Atherosclerosis: the road ahead. Cell 104: 503-516

Glukhova MA, Frid MG, Shekhonin BV, Vasilevskaya TD, Grunwald J, Saginati M, Koteliansky VE (1989) Expression of extra domain A fibronectin sequence in vascular smooth muscle cells is phenotype dependent. J. Cell Biol. 109: 357-366

Goldbourt U, Neufeld HN (1986) Genetic aspects of arteriosclerosis. Arteriosclerosis 6: 357-377

Hahn C, Schwartz MA (2008) The role of cellular adaptation to mechanical forces in atherosclerosis. Arterioscler. Thromb. Vasc. Biol. 28: 2101-2107

Hahn C, Schwartz MA (2009) Mechanotransduction in vascular physiology and atherogenesis. Nat. Rev. Mol. Cell Biol. 10: 53-62

Hahn C, Orr AW, Sanders JM, Jhaveri KA, Schwartz MA (2009) The subendothelial extracellular matrix modulates JNK activation by flow. Circ. Res. 104: 995-1003

Hynes RO (2002) Integrins: bidirectional, allosteric signaling machines. Cell 110: 673-687

Kobayashi M, Inoue K, Warabi E, Minami T, Kodama T (2005) A simple method of isolating mouse aortic endothelial cells. J. Atheroscler. Thromb. 12: 138-142

Kuhn R, Schwenk F, Aguet M, Rajewsky K (1995) Inducible gene targeting in mice. Science 269: 1427-1429

Leiss M, Beckmann K, Giros A, Costell M, Fassler R (2008) The role of integrin binding sites in fibronectin matrix assembly in vivo. Curr. Opin. Cell Biol. 20: 502-507

Libby P, Ridker PM, Hansson GK (2011) Progress and challenges in translating the biology of atherosclerosis. Nature 473: 317-325

Lusis AJ (2000) Atherosclerosis. Nature 407: 233-241

Moretti FA, Chauhan AK, Iaconcig A, Porro F, Baralle FE, Muro AF (2007) A major fraction of fibronectin present in the extracellular matrix of tissues is plasma-derived. J. Biol. Chem. 21: 28057-28062

Nakashima Y, Plump AS, Raines EW, Breslow JL, Ross R (1994) ApoE-deficient mice develop lesions of all phases of atherosclerosis throughout the arterial tree. Arterioscler. Thromb. 1: 133-140

Newby AC (2007) Metalloproteinases and vulnerable atherosclerotic plaques. Trends Cardiovasc. Med. 17: 253-258

Newby AC, Zaltsman AB (1999) Fibrous cap formation or destruction–the critical importance of vascular smooth muscle cell proliferation, migration and matrix formation. Cardiovasc. Res. 41: 345-360

Newby AC, George SJ, Ismail Y, Johnson JL, Sala-Newby GB, Thomas AC (2009) Vulnerable atherosclerotic plaque metalloproteinases and foam cell phenotypes. Thromb. Haemost. 101: 1006-1011

Ni H, Yuen PS, Papalia JM, Trevithick JE, Sakai T, Fässler R, Hynes RO, Wagner DD (2003) Plasma fibronectin promotes thrombus growth and stability in injured arterioles. Proc. Natl. Acad. Sci. 100: 2415-2419

Oh E, Pierschbacher M, Ruoslahti E (1981) Deposition of plasma fibronectin in tissues. Proc. Natl. Acad. Sci. 78: 3218-3221

Orem C, Durmuş I, Kilinç K, Baykan M, Gökçe M, Orem A, Topbaş M (2003) Plasma fibronectin level and its association with coronary artery disease and carotid intima-media thickness. Coron. Artery Dis. 14: 219-224

Orr AW, Sanders JM, Bevard M, Coleman E, Sarembock IJ, Schwartz MA (2005) The subendothelial extracellular matrix modulates NF-kappaB activation by flow: a potential role in atherosclerosis. J. Cell Biol. 169: 191-202

Orr AW, Ginsberg MH, Shattil SJ, Deckmyn H, Schwartz MA (2006) Matrix-specific suppression of integrin activation in shear stress signaling. Mol. Biol. Cell 11: 4686-4697

Orr AW, Stockton R, Simmers MB, Sanders JM, Sarembock IJ, Blackman BR, Schwartz MA (2007) Matrix-specific p21-activated kinase activation regulates vascular permeability in atherogenesis. J. Cell Biol. 176: 719-727

Orr AW, Hahn C, Blackman BR, Schwartz MA (2008) p21-activated kinase signaling regulates oxidant-dependent NF-kappa B activation by flow. Circ. Res. 103: 671-679

Ozcelik F, Erdogan O, Aktoz M, Ekuklu G, Tatli E, Demir M (2009) Diagnostic value of plasma fibronectin level in predicting the presence and severity of coronary artery disease. Ann. Hematol. 88: 249-253

Sakai T, Johnson KJ, Murozono M, Sakai K, Magnuson MA, Wieloch T, Cronberg T, Isshiki A, Erickson HP, Fässler R (2001) Plasma fibronectin supports neuronal survival and reduces brain injury following transient focal cerebral ischemia but is not essential for skin-wound healing and hemostasis. Nat. Med. 7: 324-330

Schneider A, Zhang Y, Guan Y, Davis LS, Breyer MD (2003) Differential, inducible gene targeting in renal epithelia, vascular endothelium, and viscera of Mx1Cre mice. Am. J. Physiol. Renal Physiol. 284: 411-417

Song KS, Kim HK, Shim W, Jee SH (2001) Plasma fibronectin levels in ischemic heart disease. Atherosclerosis 154: 449-453

Steiner O, Coisne C, Engelhardt B, Lyck R (2010) Comparison of immortalized bEnd5 and primary mouse brain microvascular endothelial cells as in vitro blood–brain barrier models for the study of T cell extravasation. J. Cereb. Blood Flow Metab. 31: 315-327

Tan MH, Sun Z, Opitz SL, Schmidt TE, Peters JH, George EL (2004) Deletion of the alternatively spliced fibronectin EIIIA domain in mice reduces atherosclerosis. Blood 104: 11-18

Tzanatos HA, Tseke PP, Pipili C, Retsa K, Skoutelis G, Grapsa E (2009) Cardiovascular risk factors in non-diabetic hemodialysis patients: a comparative study. Ren. Fail. 31: 91-97

Tzima E, Del Pozo MA, Kiosses WB, Mohamed SA, Li S, Chien S, Schwartz MA (2002) Activation of Rac1 by shear stress in endothelial cells mediates both cytoskeletal reorganization and effects on gene expression. EMBO J. 24: 6791-6800

Vavalle JP, Wu SS, Hughey R, Madamanchi NR, Stouffer GA (2007) Plasma fibronectin levels and coronary artery disease. J. Thromb. Haemost. 4: 864-866

White ES, Baralle FE, Muro AF (2009) New insights into form and function of fibronectin splice variants. J. Pathol. 216: 1-14

Woollard KJ, Geissmann F (2010) Monocytes in atherosclerosis: subsets and functions. Nat. Rev. Cardiol. 7: 77-86

Zhang Y, Zhou X, Krepinsky JC, Wang C, Segbo J, Zheng F (2006) Association study between fibronectin and coronary heart disease. Clin. Chem. Lab. Med. 44: 37-42

